

Type-I pseudo-first-order phase transition induced electrocaloric effect in lead-free $\text{Bi}_{0.5}\text{Na}_{0.5}\text{TiO}_3\text{--}0.06\text{BaTiO}_3$ ceramics

Feng Li, Guorui Chen, Xing Liu, Jiwei Zhai, Bo Shen, Shandong Li, Peng Li, Ke Yang, Huarong Zeng, and Haixue Yan

Citation: *Appl. Phys. Lett.* **110**, 182904 (2017); doi: 10.1063/1.4983029

View online: <http://dx.doi.org/10.1063/1.4983029>

View Table of Contents: <http://aip.scitation.org/toc/apl/110/18>

Published by the [American Institute of Physics](#)

Articles you may be interested in

[Influence of structural evolution on energy storage properties in \$\text{Bi}_{0.5}\text{Na}_{0.5}\text{TiO}_3\text{--SrTiO}_3\text{--NaNbO}_3\$ lead-free ferroelectric ceramics](#)

Appl. Phys. Lett. **121**, 054103054103 (2017); 10.1063/1.4975409

[Impact of phase transition sequence on the electrocaloric effect in \$\text{Pb}\(\text{Nb,Zr,Sn,Ti}\)\text{O}_3\$ ceramics](#)

Appl. Phys. Lett. **110**, 082901082901 (2017); 10.1063/1.4976827

[Macroscopic ferroelectricity and piezoelectricity in nanostructured \$\text{NaNbO}_3\$ ceramics](#)

Appl. Phys. Lett. **110**, 122901122901 (2017); 10.1063/1.4978904

[Enhanced energy storage density by inducing defect dipoles in lead free relaxor ferroelectric \$\text{BaTiO}_3\$ -based ceramics](#)

Appl. Phys. Lett. **110**, 132902132902 (2017); 10.1063/1.4979467

[Tuning electrical conductivity, charge transport, and ferroelectricity in epitaxial \$\text{BaTiO}_3\$ films by Nb-doping](#)

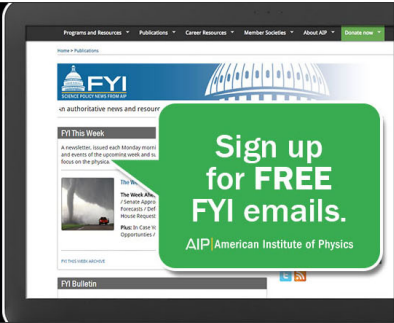
Appl. Phys. Lett. **110**, 182903182903 (2017); 10.1063/1.4982655

[Local structure of the B-site in \$\text{BNT-xBT}\$ investigated by \$^{47,49}\text{Ti}\$ NMR: Effect of barium content](#)

Appl. Phys. Lett. **121**, 114104114104 (2017); 10.1063/1.4978017



Fearful for the future of science?



Programs and Resources | Publications | Career Resources | Member Societies | About AIP | [Contact Us](#)

FYI
AMERICAN INSTITUTE OF PHYSICS

on authoritative news and resources

FYI This Week
A newsletter, issued each Monday morning and events of the upcoming week and in focus on the physics.

Sign up for FREE FYI emails.
AIP American Institute of Physics

FYI Bulletin

Type-I pseudo-first-order phase transition induced electrocaloric effect in lead-free $\text{Bi}_{0.5}\text{Na}_{0.5}\text{TiO}_3\text{--}0.06\text{BaTiO}_3$ ceramics

Feng Li,^{1,2,3,a)} Guorui Chen,^{4,a)} Xing Liu,¹ Jiwei Zhai,^{1,b)} Bo Shen,¹ Shandong Li,^{4,b)} Peng Li,¹ Ke Yang,¹ Huarong Zeng,² and Haixue Yan^{5,b)}

¹Functional Materials Research Laboratory, School of Materials Science and Engineering, Tongji University, 4800 Caoan Road, Shanghai 201804, China

²Key Laboratory of Inorganic Functional Materials and Devices, Shanghai Institute of Ceramics, Chinese Academy of Sciences, Shanghai 200050, China

³University of Chinese Academy of Sciences, Beijing 100049, People's Republic of China

⁴College of Physics, Qingdao University, 308 Ningxia Road, Qingdao 266071, China

⁵School of Engineering and Materials Science, Queen Mary University of London, London E1 4NS, United Kingdom

(Received 23 February 2017; accepted 22 April 2017; published online 2 May 2017)

In this study, the electrocaloric effect (ECE) of $\text{Bi}_{0.5}\text{Na}_{0.5}\text{TiO}_3\text{--}0.06\text{BaTiO}_3$ (BNT-0.06BT) ceramic has been directly measured using a home-made adiabatic calorimeter. The maximum adiabatic temperature change (ΔT) approaches 0.86 K under an electric field of 5 kV/mm at 110 °C, which provides experimental evidence for optimizing the ECE near the type-I pseudo-first-order phase transition (PFOPT). Most importantly, a considerable ΔT value can be maintained over a wide temperature range well above the temperature of the PFOPT under a high electric field. In addition, ΔT is closely related to the structural transition and electric field strength. This work provides a guideline to investigate the high ECE in BNT-based ferroelectric ceramics for applications in cooling technologies. Published by AIP Publishing. [<http://dx.doi.org/10.1063/1.4983029>]

Recently, triggered by microelectronics development and difficult global warming problems, the electrocaloric effect (ECE) has received considerable interest because of its potential in refrigeration applications.^{1,2} Because the ECE can be achieved by the simple operating force of an external electric field compared with the magnetocaloric/elastocaloric effect induced by large magnetism/stress, the ECE is believed to be promising for refrigeration applications.^{3–8} The ECE is the temperature variation based on the dipolar entropy change upon the application and release of an electric field. Investigation of the ECE has been revived since a colossal ECE of $\Delta T \approx 12$ K was reported in lead titanate zirconate-based antiferroelectric thin films and ferroelectric polymers.^{9,10} Inspired by these intriguing results, the ECE in a variety of ferroelectric, antiferroelectric, and relaxor materials has been extensively studied.^{7,11–13} However, for normal ferroelectrics with a first-order phase transition, a high ECE can only be obtained in a narrow temperature range in the vicinity of the ferroelectric–paraelectric phase transition, and so, relaxor ferroelectric ceramics with a wide and diffuse phase transition are preferred.^{14–16} Under this consideration, lead-free relaxor ferroelectric ceramics may be promising candidates for electrocaloric cooling.

Both the theory and experiment of the ECE have recently progressed.^{17–22} Unfortunately, there is still a lack of unified measurements to clearly understand the ECE evolution. In many cases, the ECE is not measured directly but calculated based on the thermodynamic Maxwell relation

$$\Delta T = -\frac{1}{C\rho} \int_{E_1}^{E_2} T \left(\frac{\partial P}{\partial T} \right)_E dE, \quad (1)$$

where P is the polarization, T is the temperature, E_1 and E_2 are the initial and final electric field strengths, C is the heat capacity, and ρ is the density of the material.

Unfortunately, this relation can only be strictly applied to equilibrium thermodynamic systems. When applied to multidomain or nonergodic relaxor (NER) ferroelectrics, its validity is a concern. Lu *et al.* investigated the ECE of direct and indirect experiments of relaxor ferroelectric polymers.²³ They found that there is a relatively large discrepancy between the magnitudes and temperature dependences of the two methods. Therefore, exploitation of direct measurement is important.

In this study, based on the above discussion, the ECE evolution of the lead-free ferroelectric relaxor ceramic $\text{Bi}_{0.5}\text{Na}_{0.5}\text{TiO}_3\text{--}0.06\text{BaTiO}_3$ (BNT-0.06BT) is investigated as a function of the electric field and temperature. On the one hand, large entropy changes can be expected at the pseudo-first-order phase transition (PFOPT). The concept of the type-I PFOPT was proposed by Wu *et al.* They suggest that polarization degenerates from a finite value to zero at the PFOPT temperature resulting in a positive ECE.²⁴ On the other hand, in BNT-0.06BT relaxor ferroelectric ceramics, a considerable ECE can be expected in a wide temperature range well above the ferroelectric–relaxor phase transition temperature.²⁵ The ECE of BNT-0.06BT has been reported, and BNT-0.06BT is considered to be a promising material for electrocaloric cooling.^{26–29} Unfortunately, most research of the ECE has been performed based on indirect measurements, and the ECE remains to be confirmed by direct measurements. Although the ECE in BNT-0.06BT has been

^{a)}F. Li and G. R. Chen contributed equally to this work.

^{b)}Authors to whom correspondence should be addressed. Electronic addresses: apzhai@tongji.edu.cn; lishd@qdu.edu.cn; and h.x.yan@qmul.ac.uk

measured using a modified-differential scanning calorimeter by Goupil and Turki,^{30,31} there is still a large gap between the theory and experiment, and the detailed characteristics of the type-I PFOPT of the ECE are missing. Hence, in this study, the ECE for BNT-0.06BT is determined by direct measurement with an adiabatic calorimeter to obtain insights into the ECE behavior. Based on this method, the temperature change can be directly measured, and other factors that vary with the temperature and electric field and may result in the variation of ΔT , such as heat capacity, can be ruled out. The details of procedures for fabrication and measurement of BNT-0.06BT are depicted in the [supplementary material](#).

The temperature dependences of the dielectric constant and loss tangent for unpoled and poled BNT-0.06BT are plotted as a function of the temperature (25–400 °C) and frequency (1, 10, and 100 kHz) in Figs. 1(a1 and 2)]. For the unpoled sample, strong frequency dispersion is observed at the low temperature dielectric anomaly, while no clear dispersion is observed at the dielectric constant maximum (T_m). The two dielectric anomalies can be ascribed to thermal evolution and reversible mutual transformation of the ferroelectric polar nanoregions (PNRs) with $R3c$ and $P4bm$ symmetry throughout the temperature range. However, a sharp and discontinuous peak can be clearly observed at $T_{FR} \approx 101$ °C, which can be attributed to the ferroelectric to relaxor phase transition accompanied by dissociation of the detextured ferroelectric domains into fragments.³² That is, the NER phase, which exists around room temperature in BNT-0.06BT before poling, can be irreversibly transformed into long-range ferroelectric order under the application of an electric field.³³ The dielectric measurement also confirms the phase structure transformation shown in Fig. S1 ([supplementary material](#)). The temperature dependence of the P - E loops and the corresponding J - E loops for poled BNT-0.06BT at $E = 6$ kV/mm are shown in Figs. 1(b) and 1(c[1–4]). Saturated and square P - E loops together with a sharp J - E peak (P_1) are observed (for simplicity, only the J - E loops at

$T = 20$ and 80 °C are shown here owing to their resemblance) as the temperature increase to 80 °C, indicating a dominant phase with long-range ferroelectric order (non-first cycle). As the temperature increases to 90 and 100 °C, slanted P - E loops with two split current peaks P_1 and P_2 are observed. The splitting of the current peaks has been frequently observed in $\text{Bi}_{0.5}\text{Na}_{0.5}\text{TiO}_3$ - and $\text{Bi}_{0.5}(\text{Mg}_{0.5}\text{Ti}_{0.5})\text{O}_3$ -based relaxor ferroelectrics, which is believed to correspond to the back-switching process of both the field induced nonergodic-ferroelectric P_1 and ergodic-ferroelectric P_2 phase transitions, respectively.^{34,35} When the temperature is further increased to higher than T_{FR} , slim P - E loops are observed. A single J - E peak forms during unloading together with a polarization current platform during loading, indicating the dominance of the ergodic relaxor (ER) phase. Polarization hysteresis is still present even above the ferroelectric-relaxor phase transition temperature, which indicates the relaxor nature of BNT-0.06BT ceramics.³⁶ Fig. 1(d) shows the polarization of the upper and lower branches in the first and third quadrants of the P - E loops as a function of the temperature and electric field. Here, T_{FR} is defined as the temperature where the maximum change in the polarization occurs at the zero electric field, which is close to the PFOPT and also in accordance with its dielectric properties. With the increasing electric field, T_{FR} moves to higher temperature and finally smears out (as shown by the dashed arrows), verifying that T_{FR} is a function of the electric field. That is, the PFOPT occurs at a lower electric field and gradually disappears with the increasing electric field.³⁷ Here, the critical point E_{CP} is defined as the field where the discontinuous step vanishes. Under this consideration, $E_{CP} = 2$ kV/mm. The effect of the shift of T_{FR} and appearance of E_{CP} on ECE and ζ will be discussed later.

Fig. 2 shows the temperature change signal versus time directly measured for poled BNT-0.06BT ceramic from 25 to 140 °C under the electric field of $E = 5$ kV/mm (the ECE for $E = 1$ – 4 kV/mm is shown in Fig. S2 ([supplementary material](#))), where the exothermic peaks refer to the application of

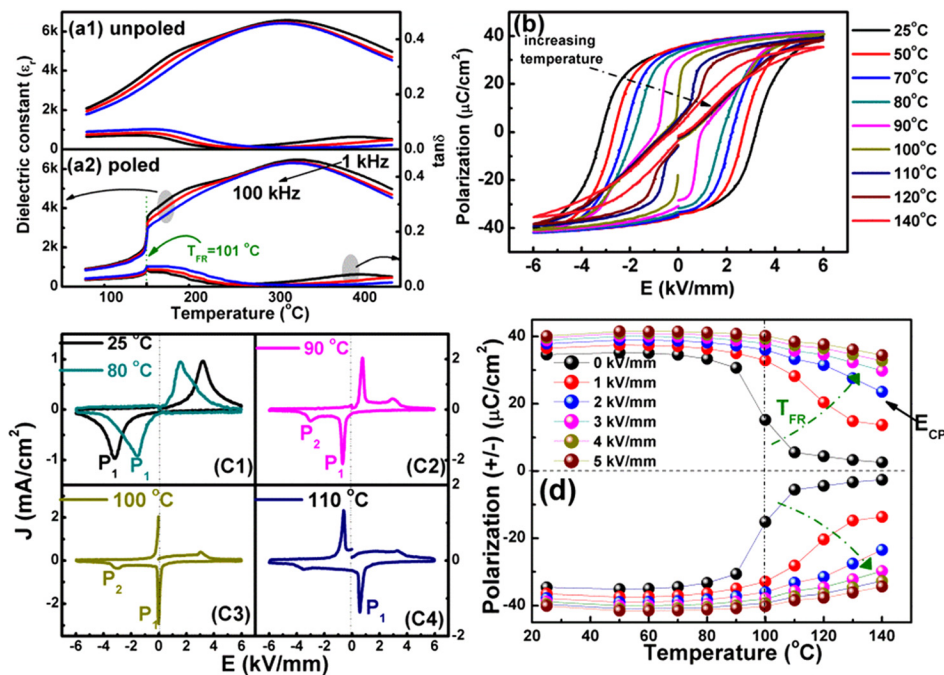


FIG. 1. (a1) and (a2) Dielectric constant of unpoled and poled BNT-0.06BT ceramics as indicated as a function of temperature and frequency; (b) P - E hysteresis loops measured at different temperatures (25–140 °C); (c) J - E loops for some specific temperatures and (d) Temperature dependence of polarization for upper and lower branch of P - E loops in first and third quadrant.

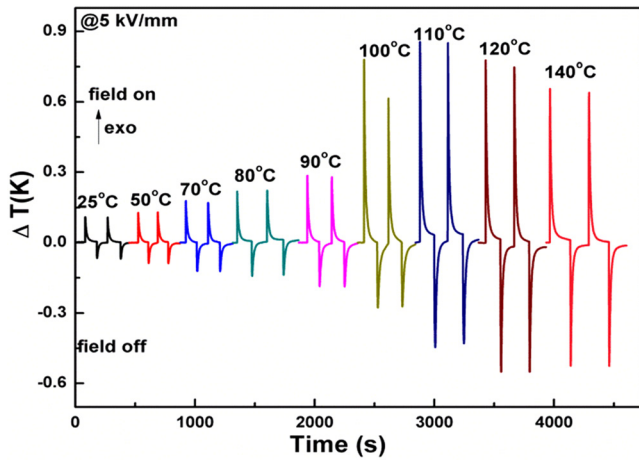


FIG. 2. A temperature change signal versus time directly measured for BNT-0.06BT from 25 to 140 °C under the electric field of $E = 5$ kV/mm.

electric fields and the endothermic peaks are because of switching off of electric fields. This phenomenon is a typical characteristic of the positive ECE. Although a negative ECE in BNT-0.06BT has been reported by indirect methods, direct measurement would be a more powerful tool to determine the nature of the ECE in BNT-0.06BT systems.^{26–29} ΔT calculated with Eq. (1) is shown in Fig. S3 (supplementary material). There is a large discrepancy between the two different methods, and the Maxwell relation is invalid for non-equilibrium conditions such as NER ceramics.²³

Fig. 3(a) shows the electric field dependence of ΔT for poled BNT-0.06BT in the temperature range of 25–140 °C, where the field-induced ΔT can be divided into two temperature regions as a function of the electric field: (I) 25–90 °C (ferroelectric order) and (II) 100–140 °C (relaxor phase). When the temperature is lower than T_{FR} , ΔT increases with increasing temperature under the same electric field and shows a linear relationship with the electric field at a certain temperature. When the temperature approaches 100 °C near

the PFOPT, a clear jump of ΔT is observed in the lower field range followed by linear evolution with the electric field in the higher field range. Fig. 3(b) shows the temperature dependence of ΔT at electric fields of $E = 1$ –5 kV/mm. The results show that there is rapid enhancement in the ECE around the PFOPT, and it remains considerable over a wide temperature range above T_{FR} under $E = 5$ kV/mm. Such a result is believed to be related to the contribution of PNR alignment induced by the electric field.¹⁵ Another interesting phenomenon is that the maximum ΔT is less dependent on the electric field, which is contrary to other BNT-based non-MPB compositions that show a pronounced field dependence.^{25,38} The strongest ECE in the low field range ($E = 1$ –4 kV/mm) occurs at or slightly below T_{FR} , while in the high electric field range ($E = 5$ kV/mm), the location of the strongest ECE moves to high temperature. For $E = 1$ kV/mm, the maximum ECE (ΔT_{max}) of 0.063 K appears at $T = 90$ °C, and it moves to $T = 100$ °C with $\Delta T_{max} = 0.44$, 0.64, and 0.76 K for $E = 2$, 3, and 4 kV/mm, respectively. When $E = 5$ kV/mm, ΔT_{max} approaches 0.86 K at $T = 110$ °C. The variation in the temperature induces a structural phase transformation from ferroelectric to the coexistence of NER and ER phases and finally to a pure ER phase with a shape change for the P - E loops, as shown in Fig. 3(b). A clear increase in the electric-field induced ECE occurs around/in the coexistence region of the NER and ER phases as a result of the maximum change in the entropy between long-range ferroelectric order induced by the electric field and the ER phase with the release of the electric field. The important parameter ξ ($\Delta T_{max}/\Delta E$) is often used to evaluate the performance of ECE materials. The critical temperature where ξ reaches a maximum is the same as ΔT . Differing from the monotonous increase in ΔT with E , the optimum value of ξ is obtained at E_{CP} , as shown in Fig. 3(d). ξ first increases from 0.063 K mm/kV at $E = 1$ kV/mm to its peak value of 0.22 K mm/kV at $E = 2$ kV/mm, and it then slowly decreases to $\xi = 0.17$ K mm/kV with the increasing electric field to $E = 5$ kV/mm at $T = 110$ °C.

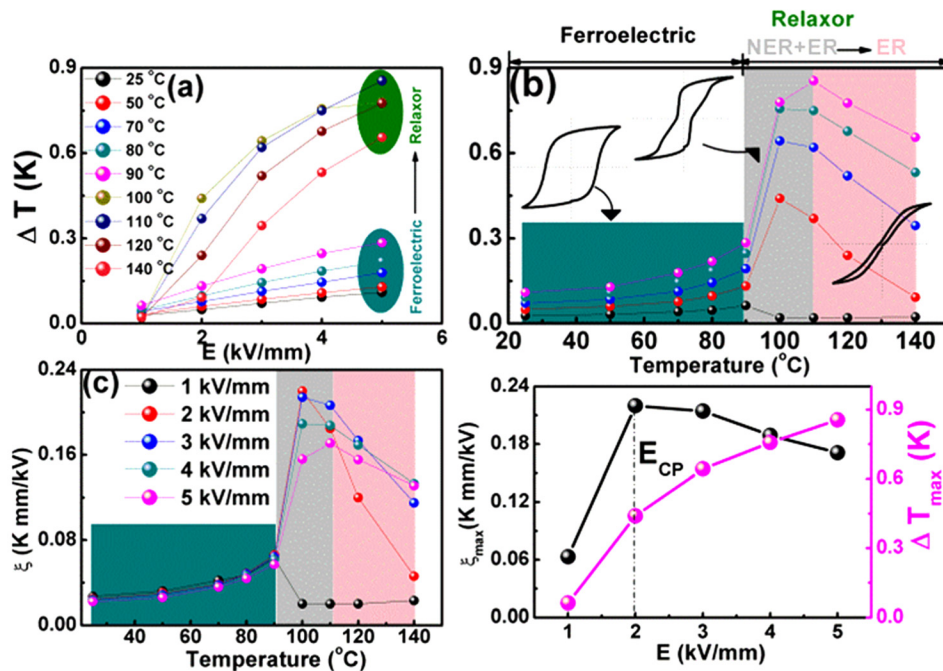


FIG. 3. (a) Electric field dependence of ΔT for BNT-0.06BT at different temperatures; Temperature dependence of (b) ΔT and (c) ξ at different electric fields; (d) the maximum value of ΔT and ξ as a function of electric field and the dash line indicates the position of E_{CP} .

A possible explanation for the decrease of ξ at a higher electric field is smearing of the PFOFT. Interestingly, the maximum values of both ΔT_{max} and ξ are achieved in the region with the coexistence of the nonergodic and ergodic phases with the PFOFT, which may provide a guideline to explore the high ECE in BNT-based ferroelectric ceramics.

To obtain insights into the underlying mechanism of ECE evolution for BNT-0.06BT in different temperature regions, a modified schematic Landau free-energy curve is delineated in Fig. 4 to reflect the evolution of the entropy and ECE as discussed above.^{15,39-41} For $T < T_{FR}$, the system is dominated by the nonergodic phase, and because $k_B T <$ local barrier, the spontaneous phase transition cannot occur. With the application of an electric field, ferroelectric order appears, and it is still dynamically stable after the release of the electric field because of the enhancement of the local barriers. In this temperature region, ΔT slowly increases as the electric field increases and a square P - E loop is observed, as shown in the cyan part of Fig. 3(b). When $T \approx T_{FR}$, the free energies of the nonergodic and ergodic phases become the same. When an electric field is applied, the field-induced long-range ferroelectric order becomes more stable than the ergodic phase. However, the field induced ferroelectric order can return to its original state owing to the low local barrier, and a slanted P - E loop is observed in this temperature region, as shown in the gray part of Fig. 3(b). Such a transformation is always accompanied by a large polarization change together with a configurational entropy change. All of these results can explain the appearance of the maximum ECE in this temperature region. When $T > T_{FR}$, the ergodic phase is dominant. The free energy of the field-induced polar phase is lower than that of the ergodic phase with the application of an electric field, and the field-induced polar phase can return to its original state with appearance of a slim P - E loop, as shown in the magenta part of Fig. 3(b). However, the entropy change in the $T > T_{FR}$ region is lower than that at $T \approx T_{FR}$, resulting in a decrease in ΔT with further increasing temperature. From the above discussion, it can be concluded that the evolution of the ECE is closely related to the structural phase transition and electric field strength.

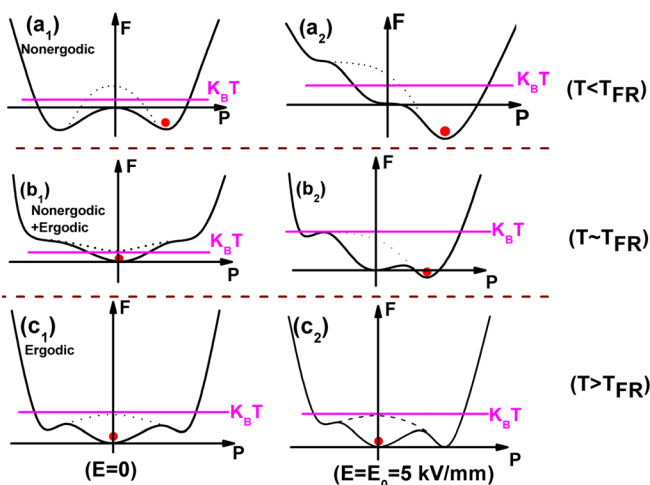


FIG. 4. Schematic Landau free-energy curves at $E = 0$ and $E = E_0 = 5$ kV/mm for three different regions: $T < T_{FR}$, $T \approx T_{FR}$ and $T > T_{FR}$.

This study is not dedicated to improving the ECE of BNT-0.06BT systems. The emphasis of this research is to directly study the ECE of an interesting family of materials, with the aim of obtaining insights into the underlying mechanisms behind the high ECE and enriching the knowledge of the ECE in BNT-based ferroelectric relaxor ceramics.

In summary, the ECE in BNT-0.06BT is reported by direct measurements, and the maximum $\Delta T_{max} = 0.86$ K is achieved in the vicinity of T_{FR} with the PFOFT. Furthermore, ξ has a maximum value of 0.22 K mm/kV at E_{CP} . Most importantly, ΔT remains considerable (≥ 0.65 K) in a wide temperature range higher than T_{FR} , which can be ascribed to the contributions of the PNRs. The results obtained in this work show that bulk BNT-0.06BT ferroelectric relaxor ceramics have great potential in refrigeration applications, and they also provide a guideline to explore a high ECE in BNT-based ferroelectric ceramics.

See [supplementary material](#) for the experimental procedure, XRD and SEM of BNT-0.06BT, temperature change signal versus time directly measured for BNT-0.06BT from 25 to 140°C under electric fields of $E = 1$ – 4 kV/mm, and results of the electric field dependence of ΔT for BNT-0.06BT at different temperatures by the indirect method.

This work was supported by Shanghai Municipal Science and Technology Commission funded international cooperation project under No. 16520721500 and the National Key R&D Program of China (2016YFA0201103). The author S. D. Li thanks the National Natural Science Foundation of China (No. 11674187). The author F. Li thanks Dr. Wanli Zhao and Hongcheng Gao for useful discussions.

- ¹J. F. Scott, *Science* **315**, 954 (2007).
- ²M. Valant, *Prog. Mater. Sci.* **57**, 980 (2012).
- ³S. G. Lu and Q. M. Zhang, *Adv. Mater.* **21**, 1983 (2009).
- ⁴A. K. Axelsson, F. L. Goupil, M. Valant, and N. M. Alford, *Acta Mater.* **124**, 120 (2017).
- ⁵Y. Bai, G. P. Zheng, and S. Q. Shi, *Appl. Phys. Lett.* **96**, 192902 (2010).
- ⁶J. T. Li, Y. Bai, S. Q. Qin, J. Fu, R. Z. Zuo, and L. J. Qiao, *Appl. Phys. Lett.* **109**, 162902 (2016).
- ⁷F. L. Goupil, A. Berenov, A. K. Axelsson, M. Valant, and N. M. Alford, *J. Appl. Phys.* **111**, 124109 (2012).
- ⁸H. Khassaf, J. V. Mantese, N. B. Gharb, Z. Kutnjak, and S. P. Alpay, *J. Mater. Chem. C* **4**, 4763 (2016).
- ⁹A. S. Mischenko, Q. Zhang, J. F. Scott, R. W. Whatmore, and N. D. Mathur, *Science* **311**, 1270 (2006).
- ¹⁰B. Neese, B. J. Chu, S. G. Lu, Y. Wang, E. Furman, and Q. M. Zhang, *Science* **321**, 821 (2008).
- ¹¹Y. Bai, D. Wei, and L. J. Qiao, *Appl. Phys. Lett.* **107**, 192904 (2015).
- ¹²L. H. Luo, M. Dietze, C. H. Solterbeck, M. E. Souini, and H. S. Luo, *Appl. Phys. Lett.* **101**, 062907 (2012).
- ¹³B. Peng, H. Q. Fan, and Q. Zhang, *Adv. Funct. Mater.* **23**, 2987 (2013).
- ¹⁴Y. Zhao, X. H. Hao, and Q. Zhang, *J. Mater. Chem. C* **3**, 1694 (2015).
- ¹⁵J. N. Li, D. W. Zhang, S. Q. Qin, T. Y. Li, M. Wu, D. Wang, Y. Bai, and X. J. Lou, *Acta Mater.* **115**, 58 (2016).
- ¹⁶J. Koruza, B. Rožič, G. Cordoyiannis, B. Malič, and Z. Kutnjak, *Appl. Phys. Lett.* **106**, 202905 (2015).
- ¹⁷I. Ponomareva and S. Lisenkov, *Phys. Rev. Lett.* **108**, 167604 (2012).
- ¹⁸B. Li, W. J. Ren, X. W. Wang, H. Meng, X. G. Liu, Z. J. Wang, and Z. D. Zhang, *Appl. Phys. Lett.* **96**, 102903 (2010).
- ¹⁹H. H. Wu, J. M. Zhu, and T. Y. Zhang, *RSC Adv.* **5**, 37476 (2015).
- ²⁰J. Wang, M. Liu, Y. J. Zhang, T. Shimada, S. Q. Shi, and T. Kitamura, *J. Appl. Phys.* **115**, 164102 (2014).
- ²¹G. Akcay, S. P. Alpay, G. A. Rossetti, Jr., and J. F. Scott, *J. Appl. Phys.* **103**, 024104 (2008).

- ²²S. P. Alpay, J. Mantese, S. Trolier-McKinstry, Q. M. Zhang, and R. W. Whatmore, *MRS Bull.* **39**(12), 1099 (2014).
- ²³S. G. Lu, B. Rožič, Q. M. Zhang, Z. Kutnjak, R. Pirc, M. R. Lin, X. Y. Li, and L. Gorný, *Appl. Phys. Lett.* **97**, 202901 (2010).
- ²⁴H. H. Wu, J. M. Zhu, and T. Y. Zhang, *Nano Energy* **16**, 419 (2015).
- ²⁵F. L. Goupil and N. M. Alford, *APL Mater.* **4**, 064104 (2016).
- ²⁶Q. Li, J. Wang, L. T. Ma, H. Q. Fan, and Z. Li, *Mater. Res. Bull.* **74**, 57 (2016).
- ²⁷X. C. Zheng, G. P. Zheng, Z. Lin, and Z. Y. Jiang, *J Electroceram.* **28**, 20 (2012).
- ²⁸G. P. Zheng, S. Uddin, X. C. Zheng, and J. H. Yang, *J. Alloys Compd.* **663**, 249 (2016).
- ²⁹Y. Bai, G. P. Zheng, and S. Q. Shi, *Mater. Res. Bull.* **46**, 1866 (2011).
- ³⁰F. L. Goupil, R. McKinnon, V. Koval, G. Viola, S. Dunn, A. Berenov, H. X. Yan, and N. M. Alford, *Sci. Rep.* **6**, 28251 (2016).
- ³¹O. Turki, A. Slimani, L. Seveyrat, G. Sebald, V. Perrin, Z. Sassi, H. Khemakhem, and L. Lebrun, *J. Appl. Phys.* **120**, 054102 (2016).
- ³²W. Jo, S. Schaab, E. Sapper, L. A. Schmitt, H. J. Kleebe, A. J. Bell, and J. Rödel, *J. Appl. Phys.* **110**, 074106 (2011).
- ³³A. A. Bokov and Z. G. Ye, *J. Mater. Sci.* **41**, 31 (2006).
- ³⁴F. Li, R. Z. Zuo, D. G. Zheng, and L. T. Li, *J. Am. Ceram. Soc.* **98**(3), 811 (2015).
- ³⁵W. L. Zhao, R. Z. Zuo, J. Fu, and M. Shi, *J. Eur. Ceram. Soc.* **34**, 2299 (2014).
- ³⁶L. E. Cross, *Ferroelectrics* **151**, 305 (1994).
- ³⁷B. Rožič, M. Kosec, H. Uršič, J. Holc, B. Malič, Q. M. Zhang, R. Blinc, R. Pirc, and Z. Kutnjak, *J. Appl. Phys.* **110**, 064118 (2011).
- ³⁸F. L. Goupil, J. Bennett, A. K. Axelsson, M. Valant, A. Berenov, A. J. Bell, T. P. Comyn, and N. M. Alford, *Appl. Phys. Lett.* **107**, 172903 (2015).
- ³⁹D. Wang, X. Q. Ke, Y. Z. Wang, J. H. Gao, Y. Wang, L. X. Zhang, S. Yang, and X. B. Ren, *Phys. Rev. B* **86**, 054120 (2012).
- ⁴⁰Y. Wang, X. Ren, K. Otsuka, and A. Saxena, *Acta Mater.* **56**, 2885 (2008).
- ⁴¹D. W. Zhang, Y. G. Yao, M. X. Fang, Z. D. Luo, L. X. Zhang, L. L. Li, J. Cui, Z. J. Zhou, J. H. Bian, X. B. Ren, and Y. D. Yang, *Acta Mater.* **103**, 746 (2016).